

See discussions, stats, and author profiles for this publication at: <https://www.researchgate.net/publication/231652503>

# Electrogenerated Chemiluminescence of Aromatic Hydrocarbon Nanoparticles in an Aqueous Solution†

ARTICLE *in* THE JOURNAL OF PHYSICAL CHEMISTRY C · JULY 2009

Impact Factor: 4.77 · DOI: 10.1021/jp901038h

---

CITATIONS

31

---

READS

29

2 AUTHORS, INCLUDING:



Khalid Omer

University of Sulaimani

12 PUBLICATIONS 248 CITATIONS

SEE PROFILE

# Electrogenerated Chemiluminescence of Aromatic Hydrocarbon Nanoparticles in an Aqueous Solution<sup>†</sup>

Khalid M. Omer and Allen J Bard\*

Center for Electrochemistry, Department of Chemistry and Biochemistry, Center for Nano- and Molecular Science and Technology, The University of Texas at Austin, Austin, Texas 78712

Received: February 4, 2009; Revised Manuscript Received: March 16, 2009

We report the preparation, characterization, and electrogenerated chemiluminescence (ECL) of rubrene nanoparticles (NPs) and 9,10-diphenylanthracene (DPA) nanorods. The organic NPs were prepared in an aqueous phase using a simple reprecipitation method, i.e., injecting a solution of the hydrocarbon in an organic solvent into water. The resulting NPs can be collected and redispersed to form stable colloidal solutions in water. Rubrene forms spherical nanoparticles (NPs) (diameter  $\sim 50$  nm), while DPA initially forms nanorods with an average size of  $\sim 500$  nm in length and  $\sim 50$  nm in diameter. DPA nanorods grew gradually with time into wires with diameters of  $\sim 1$   $\mu$ m and lengths of  $\sim 10$   $\mu$ m. ECL emission from these NPs was observed upon electrochemical oxidation in aqueous solutions containing different co-reactants, such as tri-*n*-propylamine for rubrene and an oxalate ion for DPA NPs. The ECL intensity from rubrene NPs was significantly higher than that from DPA NPs because of the smaller size, and thus there is a higher diffusion coefficient for rubrene as compared to that of DPA NPs.

## Introduction

We report electrogenerated chemiluminescence (ECL) from dispersed (colloidal solutions) of nanoparticles (NPs) of aromatic hydrocarbon compounds in an aqueous medium. Aromatic hydrocarbons in nonaqueous solvents like acetonitrile, under conditions of very small water and oxygen concentrations, were some of the earliest species studied by ECL.<sup>1</sup> However, the low solubility of aromatic hydrocarbons in water and high reactivity of their radical ions with water have prevented their investigations in aqueous media. It was of interest to see if NPs, which have sizes (in the nanometer regime) between those of molecules and bulk crystals and often exhibit characteristics different from those observed in the corresponding bulk materials,<sup>2</sup> would produce ECL. In general, organic NPs might have practical applications because their fluorescence spans a wide wavelength region, and NPs of these can be prepared with a range of sizes and shapes.<sup>3</sup> Compared to inorganic NPs, fewer studies have been conducted on the properties of organic NPs, e.g., on the size effect of organic NPs on their spectroscopic and other properties.<sup>2</sup> ECL has been extensively studied for organic molecules,<sup>1</sup> but only relatively few studies have been done on semiconductor NPs.<sup>4</sup> To our knowledge, there has been no report on ECL of organic compound NPs, probably because their nucleation and growth mechanisms are less understood and the basic properties, e.g., effect of NPs size on spectroscopy, are less well-established. The search for methods of controlling size, shape, and optical properties of organic NPs is still under development.<sup>5</sup>

In this report, we describe ECL from rubrene and 9,10-diphenylanthracene (DPA) NPs in aqueous solutions prepared by a simple reprecipitation method, in which a small amount of organic compound in a good solvent [such as tetrahydrofuran (THF), dimethylformamide (DMF), or methyl cyanide (MeCN)] is injected rapidly and stirred vigorously into a poor solvent

(such as water), in which the organic compound has a very low solubility. Characterization of the NPs using different techniques, e.g., scanning electron microscopy (SEM), transmission electron microscopy (TEM), dynamic light scattering (DLS), UV–vis absorption, and luminescence spectroscopies are discussed.

## Experimental Section

**Synthesis of Nanoparticles.** The reprecipitation method was used for this synthesis.<sup>2</sup> Rubrene NPs were synthesized by dissolving the rubrene at a 5 mM concentration in THF and quickly injecting 100  $\mu$ L of this solution into 10 mL of deionized water under an argon atmosphere with vigorous stirring at room temperature. The resulting NP solution, after filtering through a 0.22  $\mu$ m pore-sized filter (Millex GP, PES membrane), had a clear pale red color. The same procedure was followed for the preparation of DPA NPs by using MeCN, DMF, or THF as the solvent.

**Instrumentation.** UV–vis spectra were recorded on a Milton Roy Spectronic 3000 array spectrophotometer. Fluorescence spectra were recorded on a Fluorolog-3 spectrofluorimeter (ISA-Jobin Yvon Horiba, Edison, NJ), using a 1 cm path length quartz cuvette. Scanning electron microscopy (SEM) was performed with a LEO 1450VP microscope at an accelerating voltage of 20 kV and linked with an Oxford Instruments X-ray analysis system. Transmission electron microscopy (TEM) analysis and selected area electron diffraction (SAED) were conducted using a JEOL 2100F microscope at an accelerating voltage of 200 kV. Fluorescence imaging was carried out with an inverted optical microscope (Model TE 300, Nikon), and images of the emission were taken with a Model 7404-0001, Roper Scientific, Inc. camera. Current and ECL transients were simultaneously recorded using an Autolab electrochemical workstation (Eco Chemie, The Netherlands) coupled with a photomultiplier tube (PMT, Hammamatsu R4220p) held at  $-750$  V with a high-voltage power supply (Kepco, Flushing, NY). The photocurrent produced at the PMT was converted to a voltage signal by an electrometer/high resistance system (Keithley, Cleveland, OH)

\* Corresponding author. E-mail: ajbard@mail.utexas.edu.

<sup>†</sup> Part of the "Hiroshi Masuhara Festschrift".

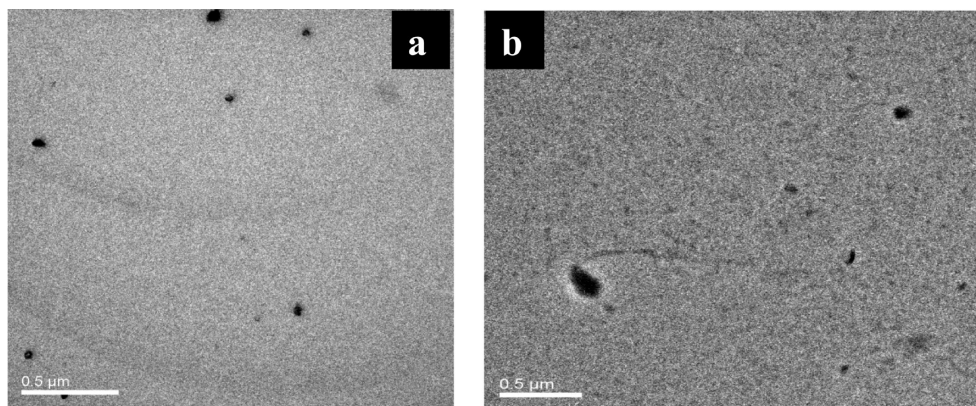


**Figure 1.** TEM images of freshly prepared rubrene NCs (a) and NCs after one week of aging in solution (b).

and fed into the external input channel of an analog-to-digital converter (ADC) of the Autolab. The electrochemical/ECL cell was composed of a J-type inlaid platinum disk as a working electrode, which was polished with alumina of different sizes between each experiment. The other electrodes were a platinum-coiled wire counter electrode and a Ag/AgCl reference electrode.

## Results and Discussion

**Microscopic and Spectroscopic Characterization.** Figure 1 shows that rubrene NPs are fairly monodispersed with a hydrodynamic radius of about 50 nm based on dynamic light scattering (DLS) measurements (see Figure S1a of the Supporting Information). From DLS measurements, the relative standard deviation for particle size was 0.6% (for  $n = 5$ ) for the DPA NPs and 0.5% (for  $n = 5$ ) for the rubrene NPs. The sizes of rubrene NPs determined from TEM images were in good agreement with DLS measurements (Figure 1). The kinetics of formation of aggregates is determined by the interaction potential between particles, the particle size, and the flow conditions during synthesis.<sup>6</sup> Ionic additives, low molecular weight molecules such as surfactant, and neutral or charged polymers can also dramatically affect the formation process and stability of the NPs. For example, particles formed in the presence of Triton X-100 were smaller (~4 nm in diameter, according to DLS measurements, see Figure S1b of the Supporting Information), and the size distribution was narrower than in its absence. However, the presence of surfactant had a negative effect on the generation of ECL, probably because the encapsulation of a particle within a layer of surfactant decreased the electron transfer rate between the particle and the electrode. NPs of rubrene in water were unstable in ambient atmosphere under room light exposure for 10 h, while they were stable for a month in the dark (although the slow formation of aggregates was seen as shown in Figure 1).

NPs of 9,10-diphenylanthracene (DPA), a well-known blue ECL emitter, prepared by using THF as a solvent did not show appreciable ECL. However DPA NPs prepared with MeCN as the solvent were larger, ~250 nm, as shown in panels a and b of Figure 2 and produced appreciable ECL with oxalate as a co-reactant as discussed below. We attribute the difference in ECL behavior for THF- and MeCN-based preparations to the size and shape of the crystals formed during the nanocrystallization process, which have been attributed to the difference in the solubility of the organic compound in water (a poor solvent) and the polarity of the good solvent. A more detailed characterization of the shape of the DPA NPs was revealed by SEM and TEM. As shown in Figure 2, DPA nanorods (50 nm in diameter and 500 nm in length) were initially formed. These

changed with time, and after about one week were converted into larger nanowires, about 1  $\mu\text{m}$  in diameter and 10  $\mu\text{m}$  in length. This shape change might be attributed to crystal-to-crystal photodimerization, which has been proposed to explain the observed shape changes in organic NPs.<sup>7</sup>

DPA nanorods deposited on a glass substrate were used to examine the fluorescence image of individual rods with fluorescence microscopy (Figure 2c,d). Under UV excitation, the rods produced blue fluorescence, which is characteristic of DPA emission. The dimensions of individual nanorods shown in the fluorescence image were in good agreement with the TEM image, indicating that in a freshly prepared aqueous NP solution rods are the predominant forms that grow into longer wires with time. However, Zhang et al.,<sup>8</sup> reported that nanorods of DPA are formed when a large volume of DPA/THF (~1 mL) is injected to 5 mL of water containing cetyltrimethyl ammonium bromide (CTAB). Although they reported that surfactant is necessary to get stable nanorods, in our work, surfactant gave a negative effect on ECL, so it was avoided.

Absorption spectra of both rubrene and DPA exhibited evenly spaced vibronic peaks that generally mirrored the emission spectra (Figure 3 and Figures S2–S5 of the Supporting Information). The absorption and emission spectra of rubrene NPs in water is red shifted by 5 nm, while the DPA NPs are red shifted by 10 nm compared to the those of a molecular solution in an organic solvent. This shift has been attributed to the polarizable environment of the surrounding NPs in water, which lowers the energy of the transition.<sup>9</sup>

**Electrochemistry and Electrogenerated Chemiluminescence.** Because of the limited potential window for electrochemical studies in aqueous solutions, the reduction of water generally prevents observation of the reduction of aromatic hydrocarbons, even those that are more easily reduced like rubrene NPs. Cyclic voltammograms (CV) of the dispersed organic NPs in aqueous 0.1 M NaClO<sub>4</sub>, however, displayed no distinctive features that could be clearly assigned to either the oxidation or reduction of the NPs. The lack of a measurable electrochemical signal can be attributed to the low concentration of the NPs (C), as well as their small diffusion coefficients (D) (because of their large radii) in the solution. The electrochemical current is governed by the flux of the NPs to the electrode surface, which is a function of both C and D.

However, one can obtain information about the redox behavior by observing ECL with a co-reactant. For example, the oxidation of rubrene NPs in the presence of a co-reactant, such as tri-*n*-propylamine (TPRA) or an oxalate ion, which form strong reducing agents ( $E_{\text{red}} \leq -1.7$  V versus SCE) on oxidation, has been shown to produce emission.<sup>1,10</sup> NPs could be oxidized



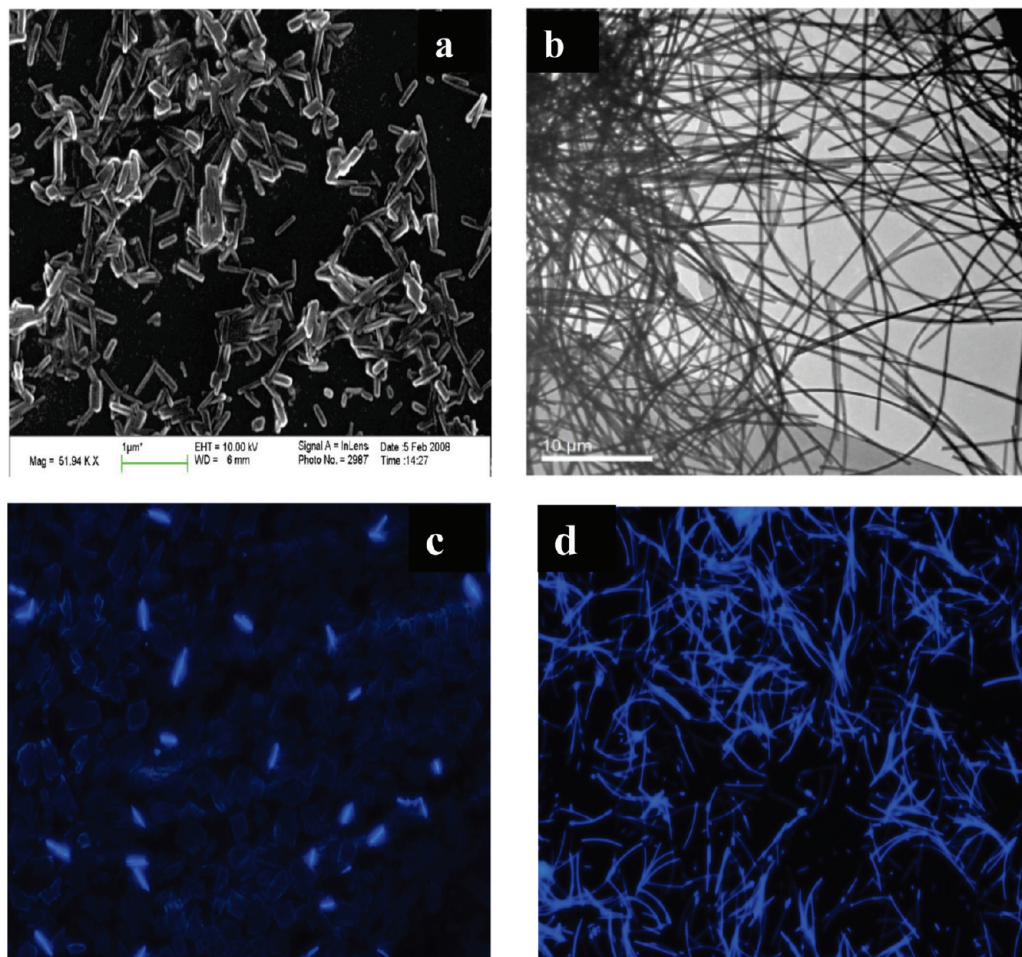


**Figure 2.** (a) SEM image of DPA nanoparticles, (b) TEM image of nanowires of DPA, (c) fluorescence image of freshly prepared DPA nanorods, and (d) fluorescence image of DPA nanowires (after one week of aging in solution).

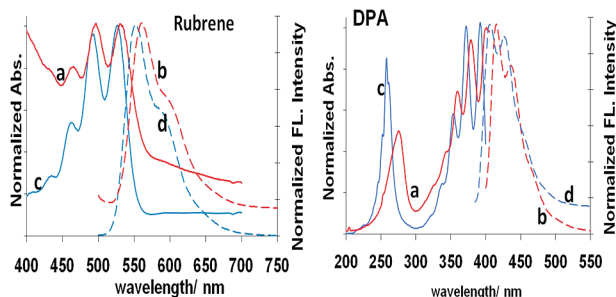


**Figure 3.** (a) Absorbance of NPs in an aqueous solution (red solid line). (b) Fluorescence of NPs in an aqueous solution (red dashed line). (c) Absorbance of rubrene dissolved in THF or DPA dissolved in MeCN (blue solid line). (d) Fluorescence of rubrene in THF or DPA in MeCN (blue dashed line).

by a potential sweep or step to a sufficiently positive potential, where the co-reactant is also oxidized. ECL emission was observed when the electrogenerated oxidized NPs ( $R^{+}$ ) reacted with the strong reducing agent (TPrA $^*$  or  $CO_2^{2-}$ ) produced by oxidation of the co-reactant to produce the excited states of NPs. The co-reactant mechanism has been described previously.<sup>10,11</sup> All of the observed electrochemical current observed in these experiments can be attributed to the co-reactant oxidation.

Transient ECL generated from the reaction of oxidized NPs and the energetic intermediate of the co-reactant was obtained by stepping the electrode potential from 0.0 V to +1.1 V versus Ag/AgCl. For rubrene NPs, as shown in Figure 4a, the ECL emission was produced when the electrode potential was stepped

to +1.1 V to oxidize both NPs and TPrA; no ECL was produced when the electrode potential was stepped back to 0.0 V. The ECL signal was sharp but weak, probably because of instabilities of the intermediates because of a reaction with water molecules and oxygen and also because of the low concentrations and diffusion coefficients of the NPs. The ECL intensity decreased with time, as shown in Figure 4d, probably because of the instability of the radical cations at the surface of the NPs. Additional ECL transients for potential steps from 0 to 0.9 V with different pulse widths are shown in Figures S6 and S7 of the Supporting Information.

The ECL versus potential curve (at a scan rate of 500 mV/s) is shown in Figure 4b, in which ECL emission was produced in the potential region where rubrene was oxidized (estimated from results in MeCN). The ECL intensity generated from rubrene NPs was strong enough to be detected with the PMT but could not be observed with the naked eye.

Poor electrochemistry was observed for NPs alone, in which the CVs were featureless. Similar behavior was found for semiconductor NPs.<sup>12,4</sup> Unlike those prepared in THF, rubrene NPs prepared in DMF produced a much smaller ECL signal that was difficult to detect at the same preparation concentration conditions (i.e., injecting 100  $\mu$ L of 1 mM rubrene in DMF into 10 mL deionized water). However, by increasing the concentration (e.g., injecting 500  $\mu$ L of 1 mM rubrene in DMF into 10 mL water), an ECL signal could be detected as shown in Figure 4c. This might be attributed to the smaller solubility

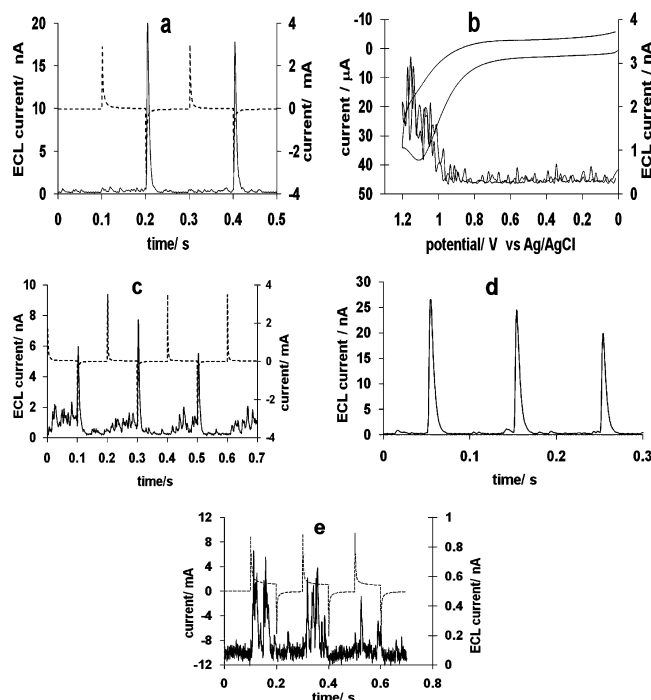


**Figure 4.** (a) Chronoamperometry (dotted line) and ECL transient (solid line) for rubrene NCs (prepared from THF) in aqueous 0.1 M TPrA and 0.1 M NaClO<sub>4</sub>, pulse width = 0.1 s. (b) Cyclic voltammogram of rubrene NCs at a scan rate of 500 mV/s. (c) Chronoamperometry (dotted line) and ECL transient (solid line) of rubrene NCs (prepared from DMF) in aqueous 0.1 M TPrA and 0.1 M NaClO<sub>4</sub>, pulse width = 0.1 s. (d) ECL transient of rubrene NCs (prepared from THF) in 0.1 M TPrA and 0.1 M NaClO<sub>4</sub>, pulse width = 0.05 s. (e) ECL (solid line) and current (dotted line) of DPA NCs in 0.1 M Na<sub>2</sub>C<sub>2</sub>O<sub>4</sub> aqueous solution.

of rubrene in DMF versus THF and the different miscibility of these two solvents with water during the reprecipitation process.<sup>13</sup>

ECL of DPA by an annihilation reaction (i.e., reaction between a cation and anion radical of DPA) in MeCN solution produces a strong blue light. As mentioned earlier, because of the limited potential window of an aqueous solution at a Pt working electrode, we are limited to studying only the oxidation of DPA in the presence of a co-reactant such as TPrA or oxalate. As reported previously in nonaqueous media,<sup>10</sup> TPrA<sup>•+</sup> is not energetic enough to generate the excited state of DPA, but oxalate is because oxalate oxidation produces the more reducing CO<sub>2</sub><sup>•−</sup> (Figure 4e). The ECL intensity was small, however, probably because of the very low diffusion coefficients of the rather large particles of DPA. The ECL intensity is governed by the flux of the NPs to the electrode, which decreases as the diffusion coefficient decreases.

In summary, ECL, particularly the co-reactant type, was produced for dispersed NPs of DPA and rubrene in aqueous media. Methods of preparation of the NPs, which in turn have effects on the nanocrystallization processes, affect the intensity of the ECL signal. Increases in intensity require formation of smaller NPs, which should produce higher concentrations and significantly larger diffusion coefficients.

## Conclusion

NPs (average radius ~50 nm) of two ECL emitters, rubrene and DPA, were synthesized and characterized. ECL of these

dispersed NPs was observed in aqueous 0.1 M NaClO<sub>4</sub> solutions containing suitable co-reactants. Rubrene formed spherical NPs, which were stable for at least one week in the dark with no significant aggregation, while DPA NPs first formed nanorods, which grew into nanowires within a week due to the instability of the initially formed NPs. The ECL intensity from the rubrene NPs was sufficient to suggest their use as labels for ECL analytical methods. However, we are attempting the preparation of smaller particles. The addition of surfactant generates smaller NPs; however, surfactant decreases the ECL intensity, probably because it interferes with electron transfer reactions at the NP surface. Alternative approaches are being investigated.

**Acknowledgment.** The authors thank Roche BioVeris, the Robert A. Welch Foundation (F-0021), and the National Science Foundation (0451494) for supporting this work. K.M.O. thanks Dr. Fu-Ren F. Fan and Dr. Dongping Zhan for helpful discussions.

**Supporting Information Available:** Contains DLS measurements, absorbance and emission spectra, transient and sweeping ECL for rubrene NPs, and SEM image for DPA NPs. This information is available free of charge via the Internet at <http://pubs.acs.org>.

## References and Notes

- (1) Reviews of ECL, see (a) *Electrogenerated Chemiluminescence*; Bard, A. J.; Ed; Marcel Dekker, Inc.; New York, 2004. (b) Miao, W. *Chem. Rev.* **2008**, *108*, 2506. (c) Richter, M. M. *Chem. Rev.* **2004**, *104*, 3003. (d) Knight, A. W.; Greenway, G. M. *Analyst* **1994**, *119*, 879. (e) Bard, A. J.; Debad, J. D.; Leland, J. K.; Sigal, G. B.; Wilbur, J. L.; Wohlstadtter, J. N. In *Encyclopedia of Analytical Chemistry: Applications, Theory and Instrumentation*; Meyers, R. A., Ed.; John Wiley & Sons: New York, 2000; vol 11, p 9842.
- (2) (a) Mori, J.; Miyashita, Y.; Oliveira, D.; Kasai, H.; Oikawa, H.; Nakanishi, H. *J. Cryst. Growth* **2009**, *311*, 553. (b) Wu, C.; Peng, H.; Jiang, Y.; McNeill, J. J. *Phys. Chem. B* **2006**, *110*, 14148. (c) Kaneko, K.; Shimada, S.; Onodera, T.; Kimura, T.; Matsuda, H.; Okada, S.; Kasa, H.; Oikawa, H.; Kakudate, Y.; Nakanishi, H. *Jpn. J. Appl. Phys* **2007**, *46*, 6893. (d) Kasai, H.; Nalwa, H. S.; Oikawa, H.; Okada, S.; Matsuda, H.; Minami, N.; Kakuta, A.; Ono, K.; Mukoh, A.; Nakanishi, H. *Jpn. J. Appl. Phys* **1992**, *31*, 1132. (e) Kasai, H.; Oikawa, H.; Okada, S.; Nakanishi, H. *Bull. Chem. Soc. Jpn* **1998**, *71*, 2597.
- (3) An, B.-K.; Kown, S.-K.; Jung, S.-D.; Park, S.-Y. *J. Am. Chem. Soc.* **2002**, *124*, 14410.
- (4) (a) Ding, Z.; Quinn, B. M.; Haram, S. K.; Pell, L. E.; Korgel, B. A.; Bard, A. J. *Science* **2002**, *296*, 1293. (b) Bard, A. J.; Ding, Z.; Myung, N. *Struct. Bonding (Berlin, Ger.)* **2005**, *118*, 1. (c) Myung, N.; Lu, X.; Johnston, K. P.; Bard, A. J. *Nano Lett.* **2004**, *4*, 183. (d) Myung, N.; Lu, X.; Ding, Z.; Bard, A. J. *Nano Lett.* **2004**, *2*, 1315. (e) Ren, T.; Xu, J.-Z.; Tu, Y.-F.; Xu, S.; Zhu, J.-J. *Electrochem. Commun.* **2005**, *7*, 5.
- (5) Fu, H.; Loo, H.; Xiao, D.; Xie, R.; Ji, X.; Yao, J.; Zhang, B.; Zhang, L. *Angew. Chem., Int. Ed.* **2002**, *41*, 962.
- (6) Horn, D.; Rieger, J. *Angew. Chem., Int. Ed.* **2001**, *40*, 4330.
- (7) Al-Kaysi, R. O.; Muller, A. M.; Bardeen, C. J. *J. Am. Chem. Soc.* **2006**, *128*, 15938.
- (8) Zhang, X.; Yuan, G.; Li, Q.; Wang, B.; Zhanh, X.; Zhang, R.; Chang, J. C.; Lee, C.-S.; Lee, S.-T. *Chem. Mater.* **2008**, *20*, 6945.
- (9) Kim, H. Y.; Bjoklund, S.-H. Lim.; Bardeen, C. J. *Langmuir* **2003**, *19*, 3941.
- (10) Lai, R. Y.; Bard, A. J. *J. Phys. Chem. A* **2003**, *107*, 3335.
- (11) (a) Miao, W.; Choi, J.-P.; Bard, A. J. *J. Am. Chem. Soc.* **2002**, *124*, 14478. (b) Zu, Y.; Bard, A. J. *Anal. Chem.* **2000**, *72*, 3223. (c) Leland, J. K.; Powell, M. J. *J. Electrochem. Soc.* **1990**, *137*, 3127. (d) Kanoufi, F.; Zu, Y.; Bard, A. J. *J. Phys. Chem. B* **2001**, *105*, 210.
- (12) Myung, N.; Bae, Y.; Bard, A. J. *Nano Lett.* **2003**, *3*, 1053.
- (13) Chung, H.-R.; Kown, E.; Oikawa, H.; Kasai, H.; Nakanishi, H. *J. Cryst. Growth* **2006**, *294*, 459.

JP901038H